

# Supercooled confined water and the Mode Coupling crossover temperature

P. Gallo<sup>†</sup>, M. Rovere<sup>†</sup>, E. Spohr<sup>‡</sup>

<sup>†</sup> *Dipartimento di Fisica “E. Amaldi”, Università “Roma Tre”,  
and Istituto Nazionale per la Fisica della Materia, Unità di Ricerca Roma Tre,  
Via della Vasca Navale 84, I-00146 Roma, Italy*

<sup>‡</sup> *Department of Theoretical Chemistry, University of Ulm,  
Albert-Einstein-Allee 11, D-89069 Ulm, Germany*

(October 24, 2018)

We present a Molecular Dynamics study of the single particle dynamics of supercooled water confined in a silica pore. Two dynamical regimes are found: close to the hydrophilic substrate molecules are below the Mode Coupling crossover temperature,  $T_C$ , already at ambient temperature. The water closer to the center of the pore (free water) approaches upon supercooling  $T_C$  as predicted by Mode Coupling Theories. For free water the crossover temperature and crossover exponent  $\gamma$  are extracted from power-law fits to both the diffusion coefficient and the relaxation time of the late  $\alpha$  region.

The effect of supercooling on the dynamics of liquids in confined environments is a research field that has become more and more popular over the last few years. Out of an extremely rich phenomenology that shows diversification of specific behavior depending on the size of the particles, the confining geometry and the specific interaction with the substrate, some general trends can none the less be extracted [1–3]. In fact two competing effects seem to be the main contributions to the modification of the dynamics of the confined liquid with respect to the bulk phase: the bare geometric confinement and the interaction with the substrate. In particular there is evidence from experiments that liquid-wall interactions can lead to a layering and a decrease of mobility close to the substrate, with a substantial increase of the glass transition temperature. This effect is stronger for attractive interactions between the substrate and the liquid. In some liquids experimental evidences show two distinct dynamical regimes [1,3].

Among liquids water plays a most fundamental role on earth. The study of the dynamics of water at interfaces or confined in nanopores as a function of temperature and hydration level is relevant in understanding important effects in systems of interest to biology, chemistry and geophysics [4,5].

In particular the single particle dynamics of water confined in nanopores have been studied by different experimental techniques such as neutron diffraction and nuclear magnetic resonance [6]. A slowing down of the dynamics with respect to the bulk phase is observed. Nevertheless the details of the microscopic dynamic behavior of confined water upon supercooling are still unclear.

Below 235 K bulk liquid water enters the so called *no man’s land* [7], where nucleation processes, most likely triggered by the presence of impurities, take place and drive the liquid to the solid crystalline phase, preventing the experimental approach to the glass phase [8,9].

The dynamical behavior of the bulk water simulated upon supercooling with the use of the Simple Point Charge/Extended (SPC/E) site model potential [10], fits in the framework of the idealized version of Mode Coupling Theory (MCT) [11], predicting a temperature of ideal structural arrest, or crossover temperature  $T_C$ , that coincides with the so called singular temperature of water [12]. This behaviour has been observed several years ago by computer simulation [13] and substantiated by experimental signatures [14] and further simulation and theoretical works [15,16]. When a liquid approaches the crossover temperature  $T_C$  MCT predicts that the dynamics is dominated by the cage effect. After an initial ballistic motion, the particle is trapped in the transient cage formed by its nearest neighbours. Once the cage relaxes the particle enters the Brownian diffusive regime. Below  $T_C$ , according to the idealized version of MCT, the system becomes non-ergodic. In real structural glasses hopping processes restore ergodicity.  $T_C$  is therefore a crossover temperature from a liquid-like to a solid-like regime. These activated processes are not relevant above  $T_C$  for most liquids.

Until now, no systematic computer simulation studies of the microscopic dynamics of confined water upon supercooling have been attempted.

Thermometric studies [17,18], NMR spectroscopy [17–20], neutron diffraction [17,21,22] and X-ray diffraction [23] show evidence that two types of water are present in the confining pores, *free water* which is in the middle of the pore and *bound water* which resides close to the surface. Free water is observed to freeze abruptly in the cubic ice structure. Bound water freezes gradually but it does not make any transition to an ice phase [23]. Layering effects of water close to the substrates have been observed in all the simulations for different geometry and water-substrate interaction [4,24].

In this letter we present evidence from Molecular Dynamics (MD) simulations that water confined in a hydrophilic nanopore exhibits two distinct dynamical regimes. In particular the fraction of free water molecules behaves similarly to the bulk phase, and its dynamics is consistent with several MCT predictions. Power law fits based on MCT yield the crossover temperature of the fraction of free water molecules; simultaneously, we show that the bound water molecules are already below  $T_C$  at room temperature.

In our simulations water has been confined in a silica cavity modeled to represent the average properties of the pores of Vycor glass [25]. Water-in-Vycor is a system of particular interest [26], since the porous silica glass is characterized by a quite narrow pore size distribution with an average diameter of 40 Å. The pore size does not depend on the hydration level and the surface of the pore is strongly hydrophilic. Moreover the water-in-Vycor system can be considered as a prototype representing more complex environments of interfacial water. Different from previous work on the dynamics of water close to a planar regular silica surface [27] we use a cylindrical geometry with a corrugated surface. We have constructed a cubic cell of silica glass by the usual quenching procedure. As described in detail in a previous work [25] inside the cube of length  $L = 71.29$  Å we cut out a cylindrical cavity of diameter 40 Å and height  $L$  by eliminating all the atoms lying within a distance  $R = 20$  Å from the axis of the cylinder, which is taken as the  $z$ -axis. After elimination of silicon atoms with less than four oxygen neighbours, we saturate the dangling bonds of oxygen atoms with hydrogen atoms, in analogy to the experimental situation [26].

Water molecules described by the SPC/E model are introduced into the cavity. The water sites interact with the atoms of the rigid matrix by means of an empirical potential model, where different fractional charges are assigned to the atomic sites of the silica glass and where the oxygen sites of water additionally interact with the oxygen atoms of the substrate via Lennard-Jones potentials [25,28]. The MD calculations are performed with periodic boundary conditions along the  $z$ -direction and the temperature is controlled via coupling to a Berendsen thermostat [29]; the shifted force method is used with a cutoff at 9 Å to truncate long-range interactions [30].

In this work we consider water at a density corresponding to the experimentally determined level of full hydration [26]. In the chosen geometry this corresponds to  $N_w = 2600$  water molecules and to a density  $\rho = 0.867$  g/cm<sup>3</sup>. We investigate the dynamical behavior of the confined water for five temperatures, namely  $T = 298, 270, 240, 220$  and 210 K.

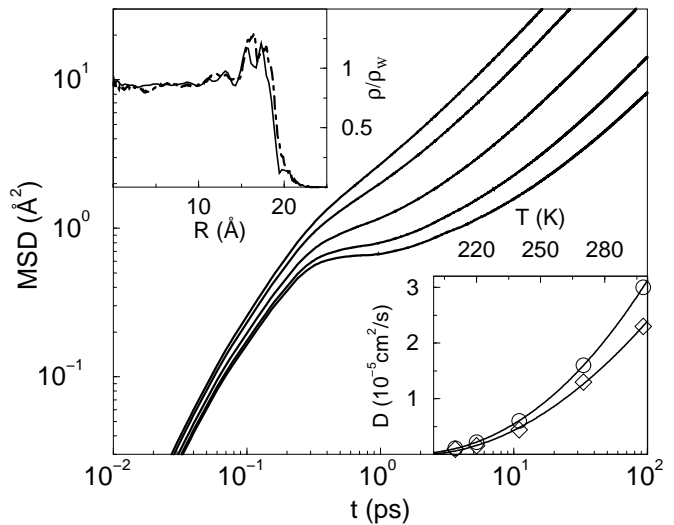


FIG. 1. Mean square displacement (MSD) along the  $z$ -direction of free water for temperatures (from top)  $T = 298, 270, 240, 220, 210$  K at full hydration ( $N_w = 2600$ ); in the upper left inset the density profiles at  $T = 298$  K (continuous line) and  $T = 210$  K (dot-dashed line) along the pore radius are shown; the lower right inset shows the diffusion coefficient  $D$  vs temperature  $T$  for the direction  $z$  (open circles) and  $xy$  (open diamonds). Full lines are power law fits to the data, given by  $D = 9.03(T/185.3 - 1)^{2.21}$  and  $D = 7.70(T/194.6 - 1)^{1.90}$  for the  $z$  and  $xy$  directions, respectively.  $D$  is in cm<sup>2</sup>/s and  $T$  is in K.

In the following we focus on the single particle dynamics of the water molecules contained in the pore and test some of the main predictions of MCT. The radial density profile of the water oxygen atoms, normalized to bulk water density, is displayed for  $T = 298$  K and  $T = 210$  K in the inset at the upper left corner of Fig. 1. It shows the high hydrophilicity of the pore in the form of density oscillations close to the substrate. These oscillations are not sensitive to supercooling. The average density of water molecules at  $T = 298$  K for  $0 < R < 15$  Å is  $\rho = 0.897$  g/cm<sup>3</sup>, for  $15 < R < 18$  Å is  $\rho = 1.079$  g/cm<sup>3</sup> and for  $R > 18$  Å (a depletion layer) is  $\rho = 0.493$  g/cm<sup>3</sup>, where  $R = \sqrt{(x^2 + y^2)}$ . In a preliminary analysis done at ambient temperature as a function of hydration level [31] we found that, due to the presence of strong inhomogeneities in our system, a fit of the total correlators to an analytic shape can be carried out only by excluding the subset of molecules in the double layer close to the substrate ( $R > 15$  Å) which we now identify with the so called bound water. In the following we show that this shell analysis keeps its validity upon supercooling. We analyze the mean square displacement (MSD) and the self intermediate scattering function (ISF) separately for bound water and for the remaining inner layers ( $R > 15$  Å), which we identify with the free water. Since no asymptotic free motion is possible in the  $xy$  plane, we separately analyze the dynamics within this plane and along the pore  $z$ -axis. In the main frame of Fig. 1 the

MSD of free water is displayed along the non-confined  $z$ -direction for the investigated temperatures. As supercooling progresses a plateau region due to the cage effect develops after the initial ballistic motion, starting around  $t = 0.3$  ps. The MSD in the  $xy$ -direction (not shown) is characterized by a similar trend, but the dynamics is slower. In the low right corner the inset shows the behavior of the diffusion coefficient  $D$  extracted from the fit of the MSD in the Brownian regime region for both the  $z$  and the  $xy$  direction together with fits of the MCT predicted power law  $D \sim (T - T_C)^\gamma$  to the 5 data points. In the  $z$ -direction, we obtain  $T_C \simeq 185.3$  K and  $\gamma \simeq 2.21$ , which are similar to the values found for the SPC/E bulk water for ambient pressure, namely  $T_C \simeq 186.3$  K and  $\gamma \simeq 2.29$  [13,32]. In the  $xy$ -direction, where the dynamics is slower, the critical temperature of free water increases to  $T_C \simeq 194.5$  K and  $\gamma \simeq 1.90$ .

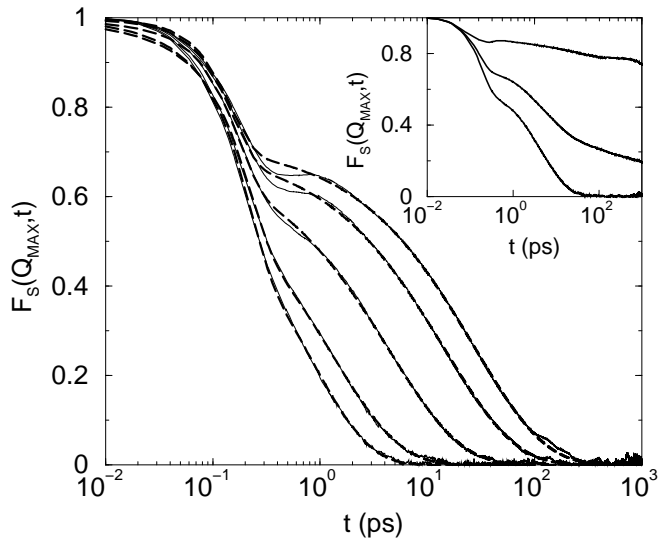


FIG. 2. Intermediate scattering function (ISF) for free water in the  $xy$ -direction at the peak of the structure factor ( $Q_{MAX} = 2.25 \text{ \AA}^{-1}$ ) for the five investigated temperatures. Curves on the top correspond to lower temperatures. Full lines are the MD data and long-dashed lines are the fit by Eq. (1). In the inset the full layer analysis is shown for  $T = 240$  K. The central curve is the total ISF, the upper curve is the bound water contribution and the lower curve is the free water contribution to the total ISF.

In Fig. 2 we show the ISF of free water at the peak of the oxygen-oxygen structure factor along the  $xy$ -direction,  $Q_{MAX} = 2.25 \text{ \AA}^{-1}$ , as a function of temperature. The free water molecules inside the pore show, similar as in SPC/E bulk water, a diversification of the relaxation times as supercooling proceeds. The plateau region stretches as  $T_C$  is approached. The long time region, the so-called late  $\alpha$  region, is expected to have a stretched exponential decay for a liquid approaching  $T_C$ . In the same figure, the fit of the function

$$F_S(Q, t) = [1 - A(Q)] e^{-(t/\tau_s)^2} + A(Q) e^{-(t/\tau_l)^\beta} \quad (1)$$

to the data points is shown, where  $A(Q) = e^{-a^2 Q^2/3}$  is the Debye-Waller factor arising from the cage effect with  $a$  the effective cage radius.  $\tau_s$  and  $\tau_l$  are, respectively, the short and the long relaxation times, and  $\beta$  is the Kohlrausch exponent. Obviously the Gaussian form of the fast relaxation can be only an approximate one.

In the inset of Fig. 2 we show the full layer analysis for  $T = 240$  K as a representative case. The topmost curve shows the behavior of bound water, while the lower curve is the ISF of free water (identical to the curve in the main picture). It is clearly seen that bound water is below  $T_C$ , since the correlation function does not decay to zero on the nanosecond time scale. The central curve is the total ISF of confined water. It displays a strong non-exponential tail, which cannot be fitted by a stretched exponential function. Our layer analysis shows clearly that the contribution of free water can be separated from the one of bound water and that the stretched exponential function is able to give a very good fit to the late part of the  $\alpha$  region in the free water subsystem as we supercool.

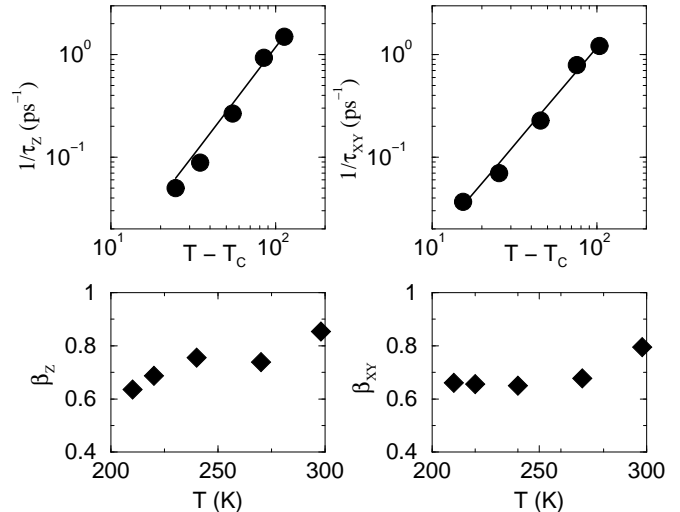


FIG. 3. The upper part of the figure shows log-log plots of the inverse relaxation times,  $\tau_l^{-1}$ , as a function of  $(T - T_C)$  along the  $z$ -direction (left) and the  $xy$  direction (right). The full lines are power law fits given by  $1/\tau_z \sim (T - 185.3)^{2.11}$  on the left and  $1/\tau_{xy} \sim (T - 194.6)^{1.90}$  on the right. The lower part shows the  $T$  dependence of the Kohlrausch exponents  $\beta$  along the  $z$  (left) and  $xy$  directions (right).

The values of the Kohlrausch exponents  $\beta$  and the relaxation times  $\tau_l$  extracted from the fits of Eq. (1) to the ISF data (Fig. 2) are reported in Fig. 3 for free water as a function of temperature for the  $z$  and the  $xy$  directions. The  $T$  dependence of  $\beta$  and  $\tau_l$  is in agreement with MCT. MCT also predicts that the inverse of the  $\alpha$ -relaxation time  $\tau_l$  vanishes with the same power law as the diffusion coefficient  $1/\tau_l \sim (T - T_C)^\gamma$ . In the upper part of Fig. 3 we show log-log plots of the inverse relax-

ation times as function of  $(T - T_C)$  as points together with power law fits as continuous lines. From the fits we obtain values very close to the ones obtained above from the power law fit of the diffusion coefficients (see inset in Fig. 1). This result seems therefore in agreement with the MCT prediction that the  $\gamma$  exponent should be independent of the quantity investigated. In pure SPC/E water the quantity  $D\tau$  was found relatively constant along isochores. None-the-less a slight increase of the product was found on cooling most likely due to the progressive breakdown of MCT on approaching  $T_C$ , see Fig. 5c of Ref. [15]. In our case a definitive conclusion on the coupling of  $D$  and  $\tau$  cannot be made at the present stage due to the fluctuations in the data. The cage radii extracted from the value of the Debye-Waller factor along both the  $xy$  and  $z$  directions range from  $a = 0.51$  Å for  $T = 298$  K to  $a = 0.45$  Å for  $T = 210$  K. The  $\tau_s$  values are  $\tau_s \sim 0.2$  ps. These values are very similar to those of SPC/E bulk water [13].

In summary, we have presented evidence that the dynamical behavior of SPC/E water confined in a silica nanopore upon supercooling can be analyzed in terms of two subsets of water molecules with clearly distinct dynamical regimes, in agreement with signatures found in experimental studies on confined liquids [1–3]. Due to the presence of a strongly attractive surface we do not find, at variance with MD studies on other confined liquids, density oscillations all over the confining space [33], or a continuous behaviour in going from the center to the substrate [34]. The bound water being close to a strong hydrophilic surface suffers a severe slowing-down already at room temperature. Power laws fit based on MCT predict that for free water ideal structural arrest would occur at  $T_C$  186.3K and 194.5 respectively along  $z$  and  $xy$  directions for the full hydration level of the pore. For the investigated quantities dynamics appears well accounted for by the idealized MCT of supercooled liquids. In this respect the predictions of the idealized MCT appear to be robust and able to describe also confined molecular liquids provided that the effects of the interaction with the substrate are properly taken into account. Experimental evidence of a possible MCT behavior of water-in-Vycor have been observed [6,35]. Therefore the analysis presented here represents an important step towards the understanding of slow structural relaxation of highly non trivial glass forming systems.

M. R. and P. G. acknowledge the financial support of the G Section of the INFM.

---

[1] J.-Y. Park and G. B. McKenna, Phys. Rev. B **61**, 6667 (2000).

[2] M. Arndt et al., Phys. Rev. Lett. **79**, 2077 (1997).  
 [3] Yu. B. Mel'nichenko, et al., J. Chem. Phys. **103**, 2016 (1995).  
 [4] R. M. Lynden-Bell and J. C. Rasaiah, J. Chem. Phys. **105**, 9266 (1996), and references therein.  
 [5] M. Settles and W. Doster, Faraday Discussion of the Chem. Soc. **103**, 269 (1996);  
 [6] J.-M. Zanotti, M.-C. Bellissent-Funel, and S.-H. Chen, Phys. Rev. E **59**, 3084 (1999), and references therein.  
 [7] H. E. Stanley, MRS Bulletin **24**, No. 5, 22 (1999).  
 [8] C. A. Angell, Ann. Rev. Phys. Chem. **34**, 593 (1983).  
 [9] P. G. Debenedetti, *Metastable Liquids: Concepts and Principles* (Princeton University Press, Princeton, 1997).  
 [10] H. J. C. Berendsen, J. R. Grigera, and T. P. Straatsma, J. Phys. Chem. **91**, 6269 (1987).  
 [11] W. Götze and L. Sjögren, Rep. Prog. Phys. **55**, 241 (1992); W. G. Götze, in *Liquids, Freezing and Glass Transition*, edited by J. P. Hansen et al. (North Holland, Amsterdam 1991).  
 [12] R. J. Speedy and C. A. Angell, J. Chem. Phys. **65**, 851 (1976).  
 [13] P. Gallo, F. Sciortino, P. Tartaglia, and S.-H. Chen, Phys. Rev. Lett. **76**, 2730 (1996); F. Sciortino, P. Gallo, P. Tartaglia, and S.-H. Chen, Phys. Rev. E **54**, 6331 (1996).  
 [14] A. P. Sokolov, J. Hurst, and D. Quitmann, Phys. Rev. B **51**, 12865 (1995); C. A. Angell, Nature **331**, 206 (1988); F. X. Prielmeir, E. W. Lang, R. J. Speedy, and H. D. Lüdemann, Phys. Rev. Lett. **59**, 1128 (1987).  
 [15] F.W. Starr, F. Sciortino and H.E. Stanley, Phys. Rev. E **60**, 6757 (1999).  
 [16] L. Fabbian et al. Phys. Rev. E **60**, 5768 (1999).  
 [17] T. Takamuku et al. J. Phys. Chem. B **101**, 5730 (1997).  
 [18] E. W. Hansen, H. C. Gran, and E. J. Sellevold, J. Phys. Chem. B **101**, 7027 (1997).  
 [19] E. W. Hansen et al., J. Phys. Chem. B **101**, 10709 (1997).  
 [20] S. Stapf and R. Kimmich, J. Chem. Phys. **103**, 2247 (1995).  
 [21] M. C. Bellissent-Funel, J. Lal, and L. Bosio, J. Chem. Phys. **98**, 4246 (1993).  
 [22] J. C. Dore, M. Dunn, and P. Chieux, J. Phys. **48**, C1 (1987); D. C. Steytler and J. C. Dore, Mol. Phys. **56**, 1001 (1985); D. C. Steytler, J. C. Dore, and C. J. Wright, J. Phys. Chem., **87**, 2458 (1983).  
 [23] K. Morishige and K. Kawano, J. Chem. Phys. **110**, 4867 (1999).  
 [24] e. g., I. Brovchenko, A. Geiger, and D. Paschek, *preprint*; A. Kohlmeyer, C. Hartnig, and E. Spohr, J. Mol. Liq. **78**, 233 (1998); J. C. Shelley et al., J. Chem. Phys. **107**, 2122 (1997); S. B. Zhu and G. W. Robinson, J. Chem. Phys. **94**, 1403 (1991); E. Spohr, J. Phys. Chem. **93**, 6171 (1989).  
 [25] E. Spohr, C. Hartnig, P. Gallo, and M. Rovere, J. Mol. Liq. **80**, 165 (1999).  
 [26] F. Bruni, M. A. Ricci, and A. K. Soper, J. Chem. Phys. **109**, 1478 (1998); A. K. Soper, F. Bruni, and M. A. Ricci, J. Chem. Phys. **109**, 1486 (1998).  
 [27] S. H. Lee and P. J. Rossky, J. Chem. Phys. **100**, 3334 (1994).  
 [28] A. Brodka and T. W. Zerda, J. Chem. Phys. **104**, 6319 (1996).  
 [29] H. J. C. Berendsen et al., J. Chem. Phys. **81**, 3684 (1984);

the Berendsen thermostat is one of the widely used and less time consuming method in computer simulation in order to control the temperature, we do not expect that our results will be any different with the use of another method.

- [30] We did check that the use of a larger cutoff or Ewald summations does not change the trend of the obtained results, see discussion in ref. [25].
- [31] P. Gallo, M. A. Ricci, M. Rovere, and E. Spohr, Euro-

phys. Lett. **49**, 183 (2000).

- [32] For values of  $T_C$  and  $\gamma$  of SPC/E water calculated over a wide range of isobars and isochores see ref. [15].
- [33] Z. T. Németh and H. Löwen, Phys. Rev. E **59**, 6824 (1999).
- [34] P. Scheidler, W. Kob and K. Binder, *preprint* cond/mat/0003257.
- [35] S.-H. Chen, P. Gallo, and M. C. Bellissent-Funel, Can. J. Phys. **73**, 703 (1995).